科学通报 2024 年 第 69 卷 第 16 期: 2157 ~ 2173
功能导向的空腔材料化学专辑 评 述
《中国科学》杂志社 SCIENCE CHINA PRESS

多级中空纳米纤维二次电池电极材料

高松伟[1], 郭威[1], 牟粤[1], 朱柯平[1], 崔志民[1], 满兴坤[2], 张千帆[3], 王女[1*], 赵勇[1*]

1. 北京航空航天大学化学学院, 仿生智能界面科学与技术教育部重点实验室, 仿生能源材料与器件北京市重点实验室, 北京 100191;
2. 北京航空航天大学物理学院, 北京 100191;
3. 北京航空航天大学材料科学与工程学院, 北京 100191
* 联系人, E-mail: wangn@buaa.edu.cn; zhaoyong@buaa.edu.cn

2023-08-25 收稿, 2023-11-19 修回, 2023-11-22 接受, 2023-11-23 网络版发表
国家自然科学基金(22175007, 21975007, 52172080)、北京市自然科学基金(2232054)和中央高校基本科研业务费专项资金资助

摘要 多级中空纳米纤维材料具有结构可控、成分可调的优点, 在二次电池电极材料领域应用广泛. 在结构方面: 多级中空结构可以有效缓冲电极材料在电化学反应离子嵌/脱过程中的体积变化, 阻止电极材料粉碎、脱落, 增加电解液和电极材料的有效接触面积, 缩短离子/电子传输路径; 在成分方面: 可以实现不同特性材料的合理耦合, 提升电极材料电导率, 加速氧化还原反应动力学. 多级中空纳米纤维结构和成分的协同增强作用在提升二次电池容量、倍率、循环性能方面效果显著. 本文归纳了现阶段制备多级中空结构纳米纤维的几类方法, 包括单针头静电纺丝、多流体静电纺丝和其他合成方法(模板法、水热法、自组装法等). 随后, 总结了不同结构、成分的纤维在二次电池(如锂、钠、钾离子电池, 锂/钠-硫电池, 锂金属-空气电池, 超级电容器等)中的应用进展. 最后, 探讨了多级中空结构纳米纤维材料在电化学储能领域的应用潜力.

关键词 多级中空结构, 纳米纤维, 异质结构, 二次电池, 电极材料

随着人类能源结构的多元化发展, 传统的化石能源如煤、石油、天然气等已无法满足人们的高质量生活需求[1,2]. 风能、水能、太阳能等新型清洁能源的发展受到了人们的极大关注, 但风能、太阳能等新型能源固有的波动性大的特性造成大量的弃电问题. 因此, 人们对大规模安全能源存储技术提出了更高的要求[3,4]. 此外, 随着便携电子设备、电动汽车的快速发展, 人们对高比能、高倍率、长循环、高安全性储能设备的需求也迅猛增长[5,6]. 二次电池在电化学储能技术中具有便携灵活、能量转换效率高和环境友好等诸多优势, 被认为是目前最具前景的能源存储技术之一[7~9]. 因此, 开发高效的新能源二次电池是实现碳达峰碳中和目标的必由之路.

二次电池由正/负极材料、电解液和隔膜组成. 其中, 高性能正负极材料的研究和开发是实现高效储能的关键. 设计具有高可逆容量、高倍率和长循环寿命的电极材料是非常必要的[10,11]. 在材料选择方面, 通常选取具有高比容量、资源丰富、环境友好的材料. 但是, 随着人们对电池高性能需求的不断提升, 研究者对于单一组分材料的研究和应用已接近其理论容量, 且无法满足电池性能的进一步改善[12,13]. 因此, 双/多组分耦合提升电池性能的设计思路已成为未来电极材料发展的必然趋势. 除组成调控外, 通过引入中空结构可以增加化学反应的有效活性位点、改善电极材料与电解液的浸润, 还可以有效缓解电极材料氧化还原反应带来的体积变化[14,15]. 因此, 通过对电极材料进行适度的中空化设计, 可以赋予电极材料保护型或功能型的外壳结构和可调的内部空间, 且中空结构电极材料具

引用格式: 高松伟, 郭威, 牟粤, 等. 多级中空纳米纤维二次电池电极材料. 科学通报, 2024, 69: 2157–2173
Gao S W, Guo W, Mu Y, et al. Multi-structure hollow nanofibers electrode materials for secondary batteries (in Chinese). Chin Sci Bull, 2024, 69: 2157–2173, doi: 10.1360/TB-2023-0887

© 2023《中国科学》杂志社

有比表面积大、离子扩散长度短、接触面积大等优点, 已广泛应用于二次电池领域[16~18]. 在各种电极材料中, 具有中空、多壁管、多孔等多级结构的纤维材料受到研究人员的广泛关注[19~21]. 多级中空结构纤维的优势在于: 一维纤维可以交织成三维多孔网络, 有利于电极材料与电解液充分接触; 中空结构可以提供合适的空隙, 缓解电极材料充放电过程中的体积变化, 防止电极材料粉碎、脱落造成的容量快速衰减; 大的比表面积提升了材料与电解液的接触, 便于电荷快速传输; 丰富的反应活性位点能极大地加速氧化还原反应活性, 缩短离子反应扩散距离, 加速反应动力学[22,23]. 此外, 多级中空纤维材料具有结构可控、成分可调的优点, 可根据应用需求合理设计具有特定结构和组成的纤维材料, 使其应用范围更加广泛[24,25]. 因此, 对多级中空纤维材料的设计、合成及应用研究对于二次电池电极的发展具有重要的意义.

本文从多级中空纤维材料入手, 对其常用的制备方法、组成结构特点、性能优势进行了总结和评述; 在此基础上, 系统地讨论了多级中空纳米纤维在二次电池(如锂、钠、钾离子电池, 锂/钠-硫电池, 金属-空气电池等)中的应用研究进展(图1)[26,27]. 最后, 对多级中空纳米纤维电极材料的发展前景进行了展望.

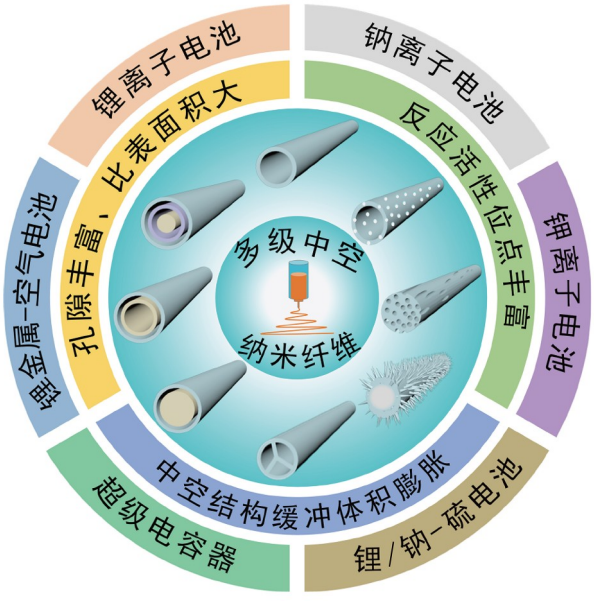


图 1 (网络版彩色)多级中空纳米纤维制备方法及二次电池应用示意图

Figure 1 (Color online) Schematic illustration of preparation methods of multi-structure hollow nanofibers and applications for secondary batteries

1 多级中空纳米纤维构筑方法

多级中空纳米纤维材料因其特有的物理化学特性, 在能源存储与转化、催化、传感等领域得到了广泛应用. 目前已经开发出多种方法合成中空纳米纤维, 如模板法、水热法、自组装法和静电纺丝等方法. 合成的多级中空结构包括中空[28]、多孔[29]、多通道[30,31]、管套线[32]、多壁管[33]、莲藕状[34]、葡萄状[35]、核壳状[36]、豆荚状[37]等(图2). 在这些方法中, 静电纺丝技术是利用高压静电力实现对纺丝溶液的喷射、拉伸细化以及固化形成纳米纤维的方法. 通过调控纺丝液组成、电纺参数、针头结构、环境参数等, 可以实现对纤维组成、形貌、结构的可控设计[38,39]. 静电纺丝技术可连续制备尺寸均一、结构可控和成分可调的复合型功能纤维材料, 被认为是制备多级中空纤维材料最有效的合成方法[40,41]. 接下来, 我们着重介绍单针头静电纺丝(简称单针电纺)和多流体静电纺丝以及其他典型方法制备具有多级中空结构纳米纤维材料.

1.1 单针头静电纺丝中空纤维

单针电纺是最简单的静电纺丝技术, 该方法装置简单、可根据需求制备具有不同直径的纤维材料. 此外, 通过调控高分子聚合物的种类、分子量、浓度等参数, 可以制备不同结构的纤维材料. 但是, 传统的单针电纺一般只能产生具有均质实心结构的纳米纤维. 近年来, 研究人员提出可以通过将单针电纺与硬模板法、乳液法、相分离法、后处理法等方法相结合产生中空结构[31,33,34,37,42~44]. 例如, 2009年, Yu等人[45]利用单针头静电纺丝技术, 以聚丙烯腈(PAN)、聚甲基丙烯酸甲酯(PMMA)和锡(Sn)前驱体纺丝液为原料, 通过热解制备出Sn颗粒封装在多通道碳纤维的电极材料. Li等人[31]利用高分子PAN和聚苯乙烯(PS)的热分解温度不同原理, 制备了多通道碳纤维. 同时, 通过调控PAN和PS的比例, 可以调控纤维通道的数量. Peng等人[43]利用单针头静电纺丝结合热处理技术制备了实心、中空、管套管纤维. 首先, 将PAN、聚乙烯吡咯烷酮(PVP)和金属盐前驱体混纺得到前驱体纤维; 随后, 通过调控热处理过程中的升温速率(高、中、低)间接调节聚合物分解速率, 得到具有不同结构的多级结构纤维. Niu等人[42]提出了梯度电纺的概念, 即利用高、中、低分子量的聚乙烯醇(PVA)在电纺纳米纤维内呈径向三层(外、中、里)分布. 热解过程中, 随着温度的缓慢升高,

内部低分子量的PVA首先热解并向低/中分子量PVA的边界移动, 同时携带无机物迁移. 接下来, 中等分子量的PVA也发生裂解, 并向高分子量的PVA层过渡, 最终形成多孔中空纤维. 单针电纺可通过控制溶液种类、溶液比例、物相析出温度等参数制备具有特殊结构的中空纤维材料.

1.2 多流体静电纺丝中空纤维

多流体静电纺丝是通过设计针头结构, 以互不相溶的两相或多相流体为内外流体, 制备具有多种组分、多种微纳结构纤维的技术. 例如, 同轴纺丝技术是将两个直径不同的针头进行同轴嵌套, 通过向两个针头分别注入两种不相溶的纺丝液体, 可以得到具有异质结构的核壳纤维, 如果选择性除去内部芯层材料, 可以得到中空纤维[28,30,46,47]. 所设计制备的纤维材料通常具有明显的中空通道、较大的比表面积、连续的三维网络等特点. 2004年, Li和Xia[28]通过同轴喷丝头设计可控制备出具备均匀壁厚的中空纤维. 2007年, 本课题组[30]通过对喷丝头的进一步改进, 提出多流体电纺技术, 制备出具有多通道结构的纤维材料. 除了制备具有不同通道数的中空纤维外, 多流体电纺技术可以根据需求, 制备不同结构类型的针头, 注入不同的溶液前驱体得到具有功能化的多级中空纤维材料. 近年来, 本课题组[46]通过同轴电纺技术制备核壳结构的CoS_2-TiO_2@C复合纤维, 外层的TiO_2和碳壳作为物理屏障限制硫和多硫化物穿梭, 内部的CoS_2作为化学吸附剂限制穿梭效应同时促进中间体多硫化物的氧化还原反应. 此外, 还利用多流体电纺设计制备了“秋葵状”多通道TiO@NC复合中空纤维用于高性能锂硫电池电极材料[47]. 纤维的通道结构有利于对硫和多硫化物的物理限域; 氮掺杂的TiO作为化学吸附“抓手”实现对硫的高效吸附和多硫化物的催化转化. 这种结合中空纤维结构和异质材料组成特性的协同设计策略对于高性能电极材料的发展至关重要.

1.3 其他合成中空纤维方法

制备多级中空纤维的方法还有模板法、水热合成法和自组装法等[48~51]. 模板法是合成中空纤维较成熟的方法之一, 通常是以天然或人工合成纤维为模板, 通过功能材料的沉积, 选择性地去除模板得到功能性的多级中空纤维材料. 水热合成法特点在于可以根据功能需求, 有选择地调变前驱体的种类和合成条件, 制备多级中空纤维. 自组装则是前驱体通过共价键等作用自发地形成稳定的、有层次的、具有特定结构(中空纤维)的组装体系. Jin等人[49]利用SiO_2中空纤维作为模板, 通过水热法制备了双壁硅酸铜中空纳米纤维. 所制备的中空纤维具有高长径比、良好的结构稳定性和高的比表面积, 可以作为催化剂的理想载体. Ding等人[50]采用室温溶液体系的氧化还原自组装法成功制备了由一维纳米槽编织而成的三维多级结构的V_6O_{13}织物, 并可通过调节前驱体浓度控制织物三维网络结构中的网孔尺寸. 这种具有多级结构的织物用作锂离子电池电极时表现出优异的结构稳定性. Fan等人[51]通过化学气相沉积法制备了由一维碳纳米纤维和二维石墨烯片组装而成的三维碳纳米纤维/石墨烯复合材料. 这种复合结构包含大量的空腔、孔隙、丰富的活性位点, 用于锂离子电池负极时表现出优异的倍率、循环性能. 这些方法在中空纤维合成的进展中也发挥着重要作用.

2 多级中空纤维在储能二次电池中的应用研究

多级中空纤维材料因具有较大的比表面积、适宜的空腔空隙和丰富的活性位点, 既能缓解充放电过程中电极材料的体积变化, 增强电极材料的循环性能, 又能增加电极材料与电解液的有效接触面积和氧化还原反应活性位点, 提高有效容量和倍率性能[52,53]. 此外, 多级中空纤维材料不仅自身可以作为电极的活性材料参与氧化还原反应, 还可以作为活性物质载体(活性物质诸如锂、钠、钾、磷、硫、硒等). 因此, 多级中空纤维材料在新型储能二次电池中应用广泛. 接下来, 我们将从应用角度出发, 分别介绍不同结构和组成的中空纤维材料在锂、钠、钾离子电池, 锂/钠-硫电池和其他新型储能体系的研究进展.

2.1 多级中空纤维在锂离子电池中的应用

锂离子电池是当前二次电池中最为广泛的电池类型, 具有能量密度高、循环性能好、环境友好等特点[54~56], 广泛应用于便携电子设备、电动汽车、储能设备等领域. 目前, 商用锂离子电池的负极材料主要由石墨类碳材料(理论容量为~372 mAh g^{-1})制成, 其制备技术成熟, 成本较低. 但是碳材料的实际容量已经达到极限[57~59], 人们一直在努力寻找具有更高理论容量的负极材料, 如合金型负极以及综合性能更加优异的金属氧化物/硫化物负极, 以取代碳质材料. 尽管新型负

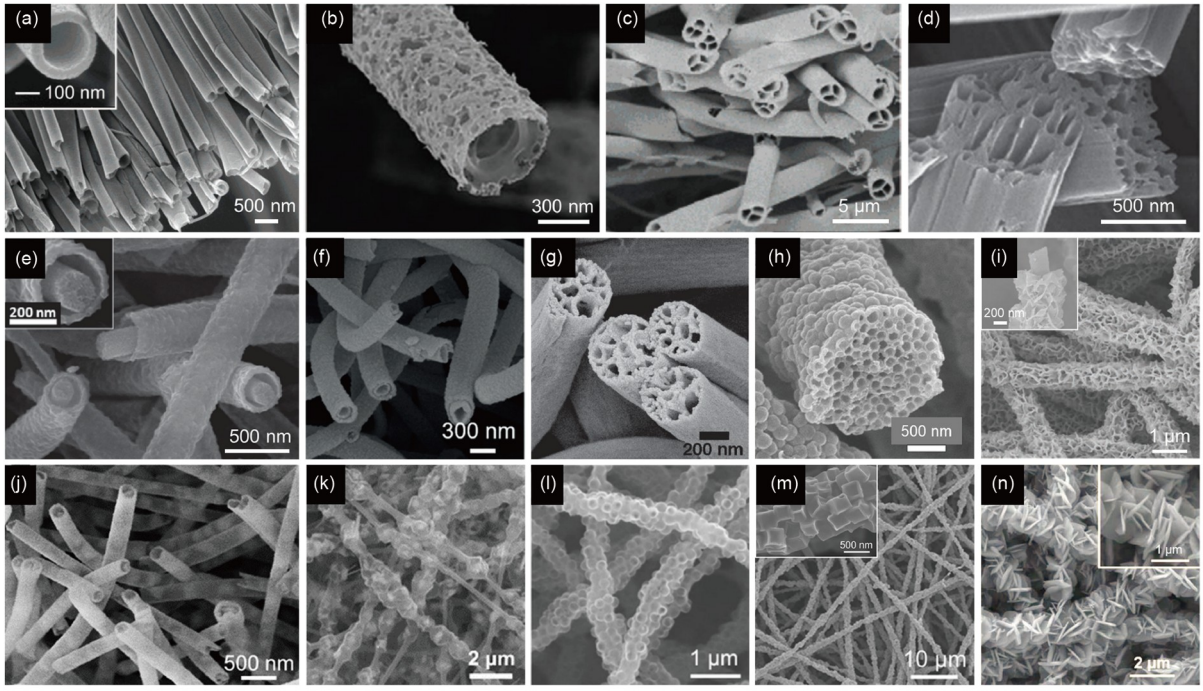


图 2 多级中空纳米纤维. (a) TiO_2中空纤维[28], Copyright©2004, American Chemical Society. (b) Co/Co_3O_4@HPCNF多孔纤维[29], Copyright©2020, John Wiley and Sons. (c) 三通道中空纤维[30], Copyright©2007, American Chemical Society. (d) 根状多通道中空纤维[31], Copyright©2017, Springer Nature. (e) 管套线γ-Fe_2O_3[32], Copyright©2010, American Chemical Society. (f) 管套管Sn/SnO_2@Carbon[33], Copyright©2020, John Wiley and Sons. (g) 多孔TiO_2中空纤维[34], Copyright©2011, John Wiley and Sons. (h) 葡萄状TiO@CHF纤维[35], Copyright©2017, Elsevier. (i) 核壳$CuCo_2S_4$ NSs@N-CNFs纤维[36], Copyright©2019, John Wiley and Sons. (j) 豆荚状中空纤维[37]. (k) 蛋黄-壳状Sb@C纳米纤维[38], Copyright©2020, John Wiley and Sons. (l) 多孔碳包覆银纳米颗粒复合纤维[39]. (m) 原子级分散的Cu和Zn位点修饰在N, P共掺杂的大孔碳纤维[40], Copyright©2023, American Chemical Society. (n) C@CoS@TiO_2分级异质纤维[41], Copyright©2019, John Wiley and Sons

Figure 2 Multi-structure hollow nanofibers. (a) TiO_2 hollow fibers[28], Copyright©2004, American Chemical Society. (b) Co/Co_3O_4@HPCNF porous fibers[29], Copyright©2020, John Wiley and Sons. (c) Three-channel hollow fibers[30], Copyright©2007, American Chemical Society. (d) Root-like multichannel hollow fibers[31], Copyright©2017, Springer Nature. (e) Fiber-in-tube γ-Fe_2O_3 fibers[32], Copyright©2010, American Chemical Society. (f) Tube-in-tube Sn/SnO_2@Carbon fibers[33], Copyright©2020, John Wiley and Sons. (g) Porous TiO_2 nanofibers[34], Copyright©2011, John Wiley and Sons. (h) Grape-cluster-like titanium monoxide@carbon hollow fiber (GC-TiO@CHF)[35], Copyright©2017, Elsevier. (i) Core-shell $CuCo_2S_4$ NSs@N-CNFs[36], Copyright©2019, John Wiley and Sons. (j) Pea-like hollow fibers[37]. (k) Yolk-shell Sb@C nanofibers (Sb@CNFs)[38], Copyright©2020, John Wiley and Sons. (l) Ag nanoparticle-embedded nitrogen doped carbon macroporous fibers (Ag@CMFs)[39]. (m) The atomically dispersed Cu and Zn sites anchored on N, P-codoped carbon macroporous fibers (Cu/Zn-N/P-CMFs)[40], Copyright©2023, American Chemical Society. (n) C@CoS@TiO_2 hierarchical heterogeneous fibers[41], Copyright©2019, John Wiley and Sons

极材料比传统石墨碳材料显示出一些优势, 但也存在一些关键的挑战, 例如: 电极材料在充放电过程中发生大的体积变化(≥ 300%)导致电极材料粉碎、团聚、脱落, 进而导致电池容量快速衰减. 此外, 缓慢的反应动力学导致其较差的容量、倍率性能[60~62]. 研究表明, 通过制备具有多级中空结构的电极材料, 能够有效改善这些问题.

Zhao等人[63]通过模板法制备了蛋黄@壳结构Bi_2S_3@N-C纳米纤维, 该纤维材料由管套线结构的活性物质Bi_2S_3芯和一个氮掺杂的介孔碳壳组成. 这种特殊的多级中空纤维用作锂离子电池负极时表现出如下优点: 中空空隙可以有效缓解Bi_2S_3纳米纤维芯较大的体积膨胀, 而不会破坏外部的保护碳壳; 原位透射电子显微镜(*in-situ* transmission electron microscope, *in-situ* TEM))表征很好地证实了这一结论(图3(a)~(f)). 外层的多孔碳壳层为Bi_2S_3芯提供了有效的电子传输路径. 此外, 碳壳层将Bi_2S_3纳米纤维芯活性材料限域在封闭的中空管内, 可以极大地防止活性材料粉碎、聚集, 从而保持整个电极材料结构的完整性. 因此, 具有多级中空结构的Bi_2S_3@N-C纳米纤维表现出优异的倍率和循环性能, 在电流密度为1 A g^{-1}时, 循环700圈后, 容量依然保持在501 mA h g^{-1}, 容量保持率为85%. Kim等人[59]通过单针头静电纺丝结合后处理法制备了Ag纳米粒子修饰的介孔SnO_2/NiO中空纳米纤维用于锂离子电池负极. 一维

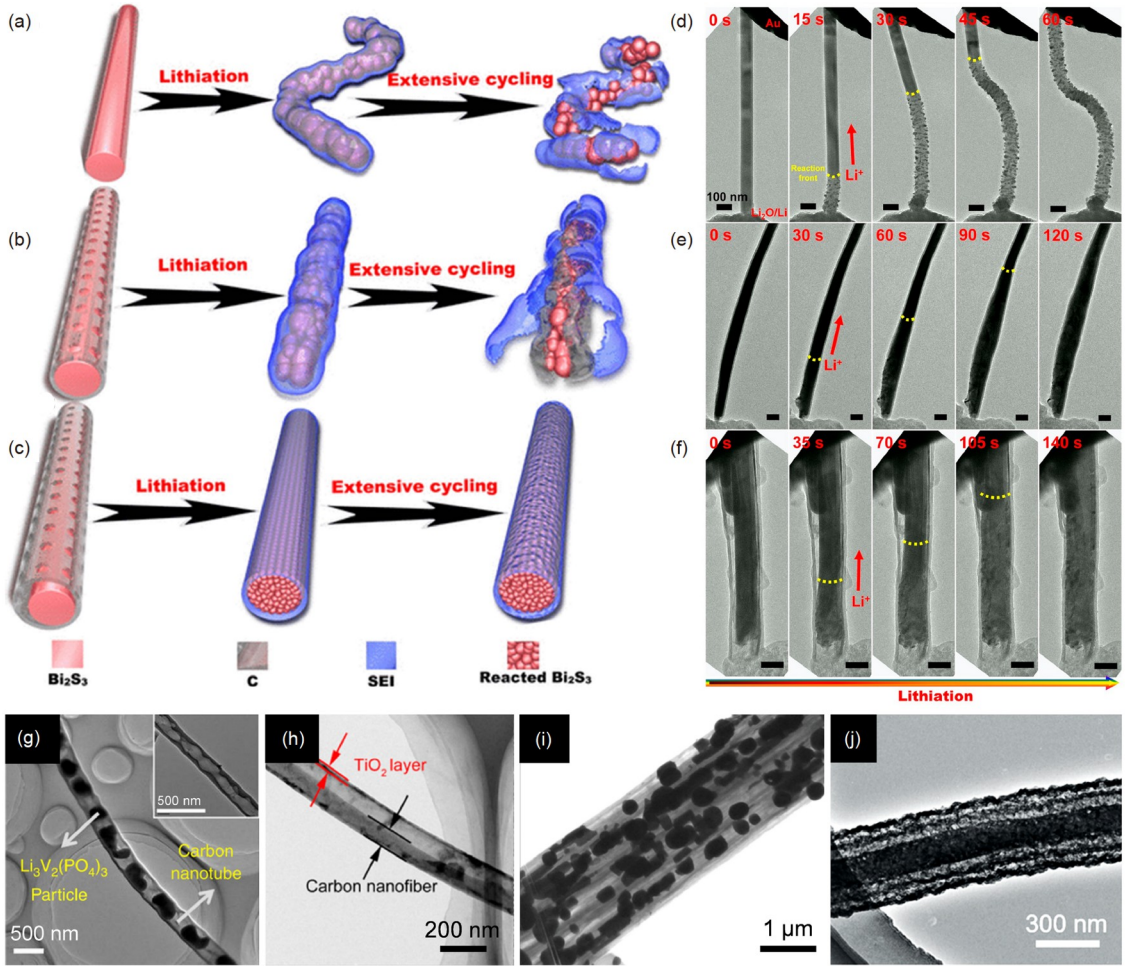


图 3 (网络版彩色)多级中空纤维用于锂离子电池. (a)~(c) 纯Bi_2S_3纳米纤维、核壳Bi_2S_3@C纳米纤维、蛋黄@壳Bi_2S_3@C纳米纤维3种负极材料的锂化过程和循环示意图[63], Copyright©2018, American Chemical Society. (d)~(f) 3种负极材料锂化过程TEM图像. (g) $Li_3V_2(PO_4)_3$豌豆状纳米管的TEM图像和用氟化氢除去$Li_3V_2(PO_4)_3$后的碳纳米管(插图)[42], Copyright©2015, Springer Nature. (h) 管套线TiO_2-Sn@C纳米纤维[64], Copyright©2017, American Chemical Society. (i) Sn颗粒分散的多通道碳纤维[45], Copyright©2009, American Chemical Society. (j) 双管套线Sn/SnO_2@C复合纤维[33], Copyright©2020, John Wiley and Sons

Figure 3 (Color online) Multi-structure hollow fibers for lithium ion batteries. (a)–(c) Schematic illustration of the lithiation process and repeated cycles of various Bi_2S_3-based anodes consisting of bare Bi_2S_3 NW, core@shell Bi_2S_3@C NW, and yolk@shell Bi_2S_3@C NW[63], Copyright©2018, American Chemical Society. (d)–(f) TEM image for three samples during the lithiation process. (g) TEM image of $Li_3V_2(PO_4)_3$ pea-like nanotube and the inset of carbon nanotubes after removing $Li_3V_2(PO_4)_3$ with hydrogen fluoride[42], Copyright©2015, Springer Nature. (h) Pipe-wire TiO_2-Sn@C nanofiber[64], Copyright©2017, American Chemical Society. (i) Sn encapsulated in multichannel carbon microtubes[45], Copyright©2009, American Chemical Society. (j) Wire-in-double-wall-tube Sn/SnO_2@C composite nanofiber[33], Copyright©2020, John Wiley and Sons

多孔中空结构有效缓解了循环过程中体积膨胀过大的问题, 并提供了较短的锂离子扩散距离. 另外, 在锂化过程中, 由NiO纳米颗粒转化而来的金属镍(Ni)纳米颗粒在氧化过程中可对Li_2O进行可逆分解, 这一作用显著提高了材料的可逆容量. 而通过简单的化学还原过程均匀修饰在SnO_2/NiO中空纳米纤维上的银纳米粒子则显著提高了倍率性能.

Niu等人[42]通过静电纺丝法制备了豆荚状的$Li_3V_2(PO_4)_3$正极材料, 由图3(g)TEM可以看出, 复合纤维呈现规整的豆荚形状. 其中, $Li_3V_2(PO_4)_3$正极活性材料均匀地分散在碳纳米管中. 与实心的$Li_3V_2(PO_4)_3$和C的复合纤维相比, 这种具有独特中空结构的电极材料呈现出更高的容量和循环稳定性. 除此之外, 研究者们还通过其他手段制备了多种多级中空结构纤维材料来提升其电化学性能.

Mao等人[64]通过模板法结合原子层沉积(atomic

layer deposition, ALD)巧妙地合成了具有管套线结构的TiO_2-Sn@C多级中空纳米纤维(图3(h)). 线主要由纳米Sn颗粒和碳纤维组成. 纳米Sn均匀地分散在碳纳米纤维中, 碳纳米纤维不仅可以防止材料的粉碎, 还可以作为导电基体, 从而提升了纤维的容量及倍率性能. 管壁是通过ALD技术沉积的TiO_2纳米管, 它作为保护壳可以有效抑制体积变化, 防止Sn活性物质在循环过程中粉碎和聚集, 从而提高了循环稳定性. Yu等人[45]通过单针头静电纺丝技术制备了多孔碳纤维包覆Sn纳米颗粒的纤维材料. 通过图3(i)中TEM可以清晰地看到, Sn颗粒均匀地分散在多孔的碳纤维中, 提升了材料的倍率和循环性能, 特别是在大电流密度下, 依然保持高的循环稳定性. 本课题组[33]通过单针头静电纺丝技术结合原位包覆和热处理过程, 制备了具有多级分层结构的双壁管套线Sn/SnO_2@Carbon异质中空纤维. 如图3(j)所示, 纤维的直径约500 nm, 呈现均匀的分层中空结构. 控制纤维的组成不变, 通过调变纤维的微/纳结构, 对比了不同结构纤维(实心、双壁管和双管套线纤维)的电化学性能. 实心纤维在循环过程中发生较大的体积变化, 纤维粉碎, 结构完整性难以保持; 双管纤维在循环过程中的纤维结构得以很好地保持, 但是过大的中空空隙降低了材料的体积比容量. 双壁管套线纤维很好地弥补了实心纤维和双管中空纤维的不足, 在容量、倍率和循环方面表现优异. 因此, 对纤维材料多级中空结构的合理构建是进一步发展高性能锂离子电池的关键.

2.2 多级中空纤维在钠离子电池中的应用

尽管锂电池的研究和商业化开发已经取得了巨大的进步, 但锂资源分布不均、可用资源短缺已经是不争的事实, 而钠资源储量丰富、价格低廉等优势明显[65~70]. 早在20世纪80年代, 钠离子电池就已经被科学家短暂研究过. 然而, 由于当时锂离子电池在能量密度方面具有明显的优势, 被广泛应用于商业化生产中, 因此, 对于钠离子电池的研究暂时被搁置. 近10年来, 由于锂资源短缺造成锂离子电池的制造成本大幅增加, 严重阻碍了其在大规模储能设备领域的发展. 而钠资源丰富且分布均匀, 因此受到了人们的青睐[71~73]. 但是, 钠离子相较于锂离子半径较大(1.02 Å vs. 0.76 Å), 原子质量更大, 因此电极反应动力学缓慢[74,75]; 同时, 在循环过程中较易产生巨大的体积膨胀, 降低电极材料的循环稳定性. 因此, 人们通过设计多级中空结构来实现高性能的钠离子电池材料的制备.

Ma等人[76]通过静电纺丝技术精准合成了富含氧空位的碳包覆SnO_{2-x}纳米粒子的纳米纤维材料, 极大地改善了钠离子电池的电化学性能. 通常人们通过将纳米SnO_2与导电基体复合来实现增强的电化学性能, 尽管这些策略能够在一定程度上抑制充放电过程中产生的体积膨胀, 加速离子/电子传输, 但它们不能保持电极的长期稳定性, 特别是在大倍率条件下的充放电过程. 这是因为纳米结构的SnO_2在电化学反应过程中会不可避免地产生裂纹, 脱离导电基体, 从而失活. 此外, Sn/Na_2O界面不稳定也是限制SnO_2基材料在钠离子电池中实际应用的主要因素. 利用氧空位等缺陷掺杂已被证明能调控氧化物半导体的电子结构, 可有效改善钠离子电池的循环和倍率性能(图4(a), (b)). 所制备的电极材料在经过2500次循环后依然稳定, 证明这种策略为制造高性能的SnO_2基电极材料开辟了新的可能途径(图4(c)). 此外, SnO_{2-x}/C复合材料能够直接用作钠离子电池负极材料, 不需要添加黏合剂和导电添加剂, 因此不仅能显著增加电池的能量密度, 而且还显示出在柔性能源存储装置中的应用前景. Pan等人[77]通过水热和模板法制备得到了层间距增加的MoS_2/C复合材料(层间距1.1 nm, 图4(d)). 层间距的扩展有利于降低钠离子的反应能垒, 加速反应动力学. 另外, 中空结构有效缓解了充放电过程中体积变化, 提升了电池的循环稳定性. Yuan等人[78]运用静电纺丝结合NH_3气氛中热解技术得到了N/F共掺杂的富含VN量子点的多孔碳纤维, 如图4(e)所示, 纤维表面均匀分散着多孔结构. 实验和理论计算证明, VN量子点与N/F共掺杂一维导电碳网络的强耦合作用有效地促进了离子/电子传递和插层-转化-脱嵌反应, 确保了钠离子的快速储存; 多孔结构中丰富的活性位点可以有效地提高钠离子的吸附/反应活性, 改善了其反应动力学. 本课题组[37]从纤维结构和组成成分协同方面入手, 通过静电纺丝和热处理技术设计制备了豆荚状MoS_2@$NiS_{1.03}$-C异质中空纤维. 如图4(f)和(g)所示, 插图为氧化物形貌图和豆荚的模型图. 纤维结构方面: 一维纳米纤维导电网络加速了电/离子传输; 多级中空结构有效缓解了钠化/脱钠过程中电极体积变化, 增大了电解液和材料的有效接触面积. 异质成分方面: 具有特殊层状结构(层间距0.62 nm)的MoS_2既能有效地贡献容量, 又能提升结构稳定性; $NiS_{1.03}$@C外壳能够有效提升材料电导率, 加速氧化还原反应动力学. 此外, 我们通过理论计算证明了异质界

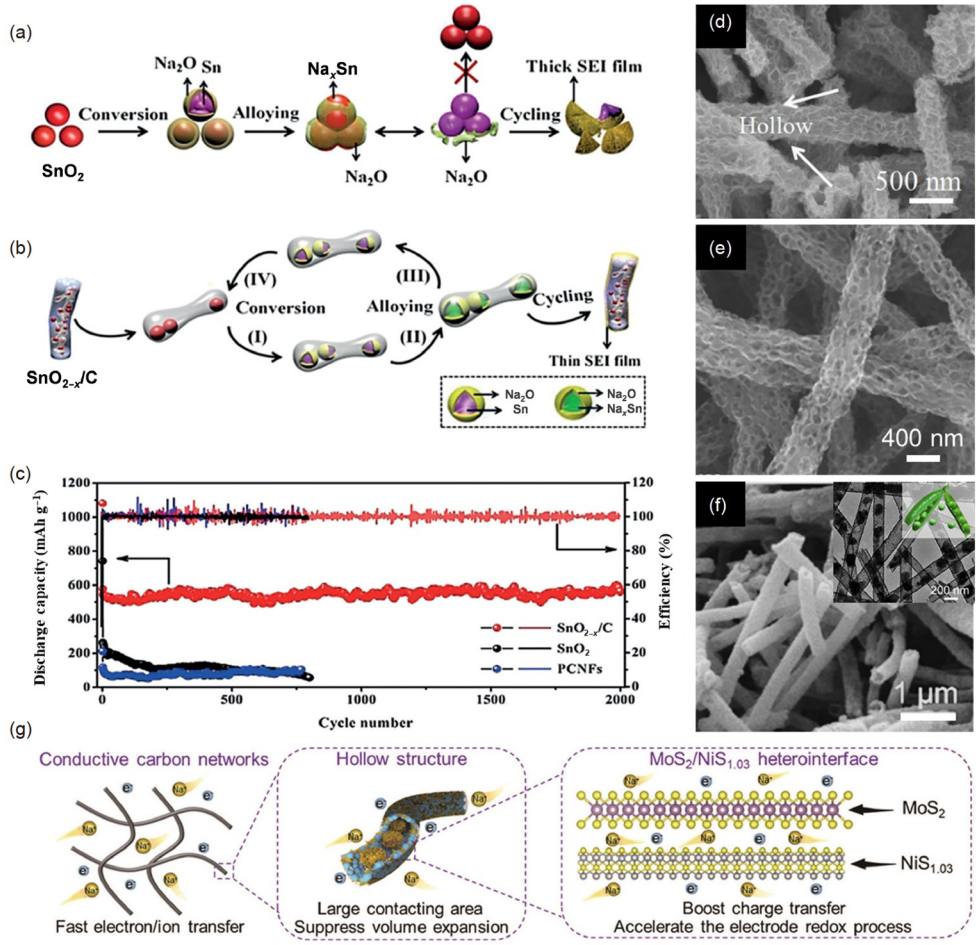


图 4 (网络版彩色)多级中空纤维用于钠离子电池. (a), (b) SnO_2和SnO_{2-x}/C电极储钠反应机理示意图[76], Copyright©2018, John Wiley and Sons. (c) 在电流密度1 A g^{-1}时, SnO_2, SnO_{2-x}/C和多孔碳纤维电极的长循环性能图. (d) MoS_2/C中空纤维[77], Copyright©2018, American Chemical Society. (e) N/F共掺杂氮化钒纤维[78], Copyright©2022, American Chemical Society. (f), (g) MoS_2@$NiS_{1.03}$-C 纳米纤维和多尺度结构与异质界面协同储钠示意图[37]

Figure 4 (Color online) Multi-structure hollow fibers for sodium ion batteries. (a), (b) The diagram of sodium storage reaction mechanisms of SnO_2 and SnO_{2-x}/C electrodes[76], Copyright©2018, John Wiley and Sons. (c) Cycling performance of SnO_2, SnO_{2-x}/C and porous carbon nanofibers (PCNFs) electrodes at current density of 1 A g^{-1}. (d) MoS_2/C hollow fibers[77], Copyright©2018, American Chemical Society. (e) N/F co-doped vanadium nitride fibers[78], Copyright©2022, American Chemical Society. (f), (g) MoS_2@$NiS_{1.03}$-C nanofibers and the schematic diagram of sodium storage with synergistic effects of multi-scale structures and heterogeneous interfaces[37]

面的设计显著降低了钠离子扩散能垒, 增强了对钠离子的吸附. 当用作钠离子电池负极时, 在电流密度5 A g^{-1}下, 循环1000圈容量保持为210 mA h g^{-1}. 以上工作证明了对纤维结构、成分的协同设计能够有效提升钠离子电池的电化学性能.

2.3 多级中空纤维在钾离子电池中的应用

与锂、钠离子电池相似, 钾离子电池同样可以作为一种新型的碱金属二次电池. 钾资源储备丰富、还原电势(−2.93 V)相较于钠(−2.71 V)更接近于锂(−3.04 V), 且钾离子在电解质中具有快速的离子传输动力学等特点, 受到了国内外学者的广泛关注[79~82]. 但是, 钾(1.38 Å)较锂和钠的离子半径更大, 导致其极差的反应动力学以及在嵌/脱钾过程中大的体积变化[83~86]. 因此, 通过结构设计对电极材料进行改性处理是钾离子电池进一步发展的有效措施. 通过合理设计多级中空结构、异质成分纤维材料, 能有效改善钾离子反应动力学缓慢和反应过程中体积变化大的问题.

Jia等人[87]通过溶剂热和退火处理得到了竹节状的MoS_2/N-doped-C纳米管. 如图5(a)~(d)所示, 这种竹节

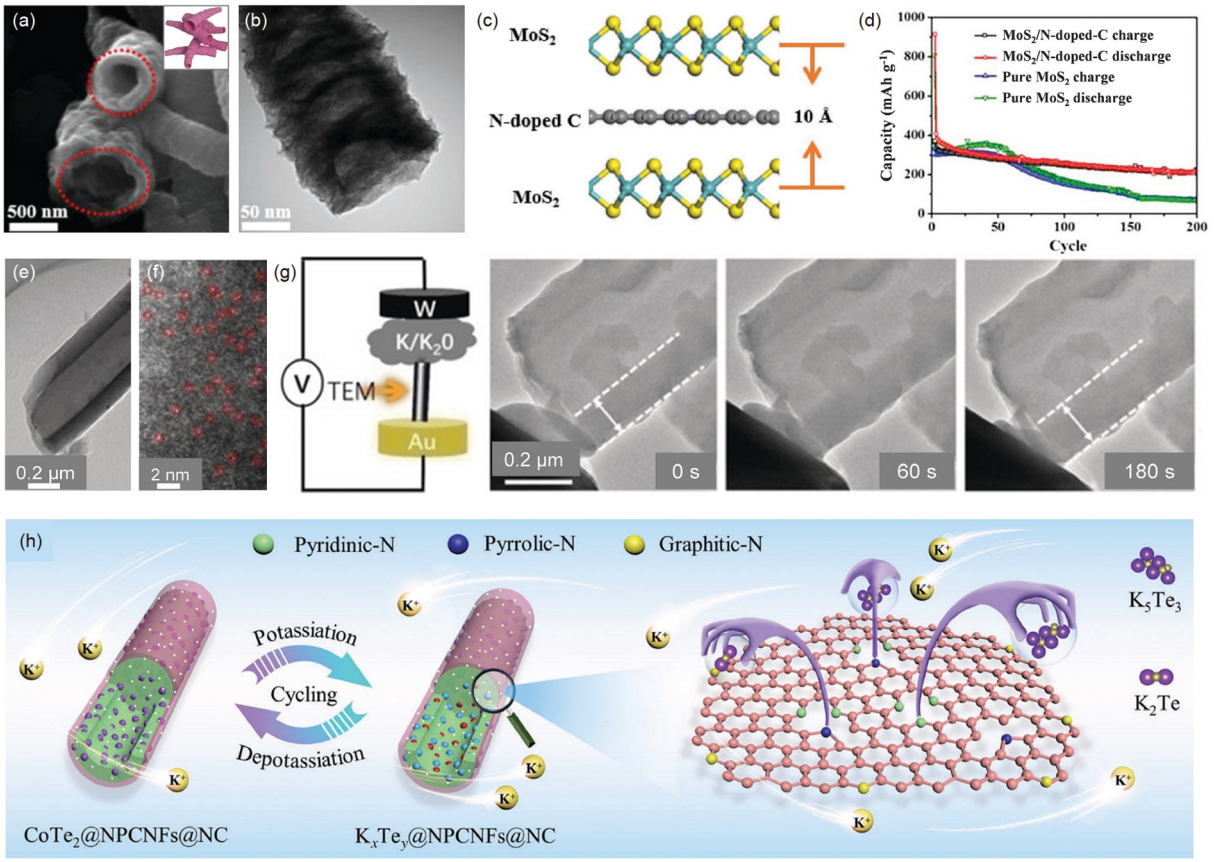


图 5 (网络版彩色)多级中空纤维用于钾离子电池. (a)~(c) MoS_2/N-doped-C中空纤维形貌及晶体结构图[87], Copyright©2018, John Wiley and Sons. (d) 纯MoS_2和MoS_2/N-doped-C中空纤维循环性能图 (e), (f) Ni SA/S/C低/高分辨率TEM图像[88], Copyright©2020, John Wiley and Sons. (g) Ni SA/S/C储钾原位TEM图. (h) $CoTe_2$@NPCNFs@NC储钾机理图[89], Copyright©2023, John Wiley and Sons

Figure 5 (Color online) Multi-structure hollow fibers for potassium ion batteries. (a)–(c) Morphology and crystalline structure of MoS_2/N-doped-C hollow fibers[87], Copyright©2018, John Wiley and Sons. (d) The cycling performances of pure MoS_2 and MoS_2/N-doped-C hollow fibers. (e), (f) Low/high-resolution TEM images of Ni SA/S/C[88], Copyright©2020, John Wiley and Sons. (g) *In-situ* TEM images of potassium storage of Ni SA/S/C. (h) The schematic graph of potassium storage of $CoTe_2$@NPCNFs@NC[89], Copyright©2023, John Wiley and Sons

状的多孔纳米管能够有效地缓解充放电过程中的体积膨胀问题; 层间距远大于钾离子半径的MoS_2(层间距10 Å), 能够极大地加速反应动力学. 与纯MoS_2相比, MoS_2/N-doped-C纳米管表现出优异的长循环稳定性, 在电流密度0.1 A g^{-1}下, 循环200圈容量为212 mA h g^{-1} (纯相MoS_2容量仅为70 mA h g^{-1}). Yi等人[88]采用以酰胺化策略为主的组装方法, 制备了一种含有单原子镍和小分子硫的碳基纳米管(图5(e)~(f)). 在制备过程中, 单原子设计和中空纳米管构筑得以同时实现. 理论计算表明, 单原子Ni可以提高碳基纳米管中化学吸附的小分子硫的反应动力学, 降低其硫化物分解能垒. 原位TEM表征表明(图5(g)), 机械稳定的中空纳米管框架能够很好地缓冲嵌/脱钾过程中的体积变化. 因此, 作为钾离子电池负极材料时, 该碳基纳米管在1.0 A g^{-1}电流密度下循环500次后, 仍保持了330.6 mA h g^{-1}的循环容量.

Li等人[89]采用静电纺丝技术、多巴胺包覆和原位碲化法合成双类型碳包覆的$CoTe_2$复合纤维材料($CoTe_2$@NPCNFs@NC). $CoTe_2$@NPCNFs@NC纳米纤维的表面没有明显暴露的颗粒, 这归功于$CoTe_2$@NPCNFs@NC的双类型N掺杂碳限域功能(其中壳聚糖衍生的碳起到吸附Co^{2+}和固定$CoTe_2$颗粒的作用, 而聚多巴胺衍生的N掺杂碳层则作为“铠甲”来稳定和限域纤维结构). 此外, 通过使用坚固的双类型N掺杂多孔碳骨架, 在充放电过程中可以有效减轻由于钾的嵌入和脱出而引起的体积变化, 从而成功地抑制了$CoTe_2$颗粒的体积效应和团聚现象. 最后, 实验验证了$CoTe_2$@NPCNFs@NC复合电极中的吡啶-N和吡咯-N碳基底

(尤其是吡咯-N)对多碲化物(K_xTe_y)具有很强的吸附作用，并且能有效抑制多碲化物中间物(K_xTe_y)在电解液中溶解，因此$CoTe_2$@NPCNFs@NC电极表现出优异的储钾性能(图5(h))．Lim等人[82]利用静电纺丝和原位热解硫化法制备了一维多通道的VS_4/碳复合材料．碳纳米纤维的多孔结构使得VS_4具有无定形特性．得益于离子/电子的快速传递、VS_4的无定形性质和碳基体的结构稳定性，VS_4/碳复合材料表现出高容量、高倍率、长循环稳定的储钾性能．

2.4 多级中空纤维在锂/钠-硫电池中的应用

近年来，由于人们对高能量密度电池需求的持续增长，对金属-硫(特别是锂/钠-硫电池)的研究备受关注．这是因为正极材料硫(S)作为锂/钠-硫电池的重要组成部分，具有高的理论比容量(1675 mA h g^{-1})．然而，硫和多硫化物较差的导电性、多硫化物在电解质中的穿梭效应、锂/钠和硫的动力学缓慢以及反应活性较差等问题限制了其进一步发展[90~95]．多级中空纳米纤维材料具有高导电性和高比表面积等优异的物理化学性能，可以作为硫有效的载体，促进电/离子快速转移并限制电极之间的多硫化物扩散．此外，可通过加入催化剂(金属单原子[96]、金属氧化物[46]、金属硫化物[97]、金属硒化物[98]、金属氮化物[99]、金属碳化物[100]等)实现对硫和多硫化物强的化学吸附作用，阻止多硫化物的穿梭．因此，对硫正极载体的合理设计被认为是实现高能量密度、长循环稳定性新型储能电池体系的有效策略．

基于这些设计理念，Li等人[101]设计了一种中空碳纳米纤维填充MnO_2纳米片的复合结构(MnO_2@HCF)，作为硫正极的高效载体(图6(a))．这种独特复合结构的优势在于碳壳对多硫化物的物理包覆以及它们与MnO_2纳米片的化学结合效应．中空碳纳米纤维易于在电极片内形成三维导电网络，有利于电/离子在充放电过程中的快速转移．同时，中空碳纳米纤维内部的MnO_2纳米片可以高效地化学结合多硫化物，有效地限制其在充放电过程中的溶解(图6(b))．MnO_2/碳/硫纳米复合电极(MnO_2@HCF/S)具有高的硫负载量(71%)、高的硫面密度(3.5 mg cm^{-2})，在不同倍率下具有很高的比容量，并且具有优异的循环稳定性(图6(c))．通过这种物理和化学方法相结合的策略，有效地提升了锂硫电池的能量密度和循环寿命．

高能量密度、长循环寿命的柔性锂硫电池是新兴的柔性、便携、可穿戴电子产品的重要组成部分．然而，由于现有的硫复合正极柔韧性差，性能衰减严重，限制了柔性锂硫电池的发展．Ma等人[102]报道了一种自支撑的高柔性硫载体，可以同时满足柔性锂硫电池的自支撑性、稳定性和容量要求．他们通过静电纺丝结合溶剂热过程，成功地合成了碳纳米管增强的“吸管状”碳包覆CoS同轴微管纳米结构(CNTs/CoS-NSs)(图6(d)~(f))．S@CNTs/CoS-NSs用作锂硫电池正极性能优异的原因在于：内部中空的纳米结构提供了较大的内部空隙，以提供高硫负载并适应硫的体积膨胀；高的局部和整体电导率以及纵横交错的三维导电网络可以降低内阻，提高硫的利用率；对硫的强化学吸附和物理约束能有效抑制穿梭效应；CoS的电催化作用有利于硫的氧化还原转化．得益于这些优点，S@CNTs/CoS-NSs正极表现出高的放电容量、倍率能力和循环稳定性．此外，基于S@CNTs/CoS-NSs作为正极的软包锂硫电池同时具有优异的柔性和高的面容量．

Ye等人[103]通过静电纺丝和氮化技术制备了多通道TiN-TiO_2@C异质中空纤维用于负载活性材料S，形成S/TiN-TiO_2@C作为室温钠硫电池的正极材料(图6(g)~(j))．在电流密度0.1 A g^{-1}时，S/TiN-TiO_2@C电极循环100圈容量仍保持640 mA h g^{-1}，库仑效率接近100%，即使在电流密度5 A g^{-1}下，经过1000次循环后，电池仍表现出257.1 mA h g^{-1}的容量．电化学分析以及第一性原理计算表明，TiN的高电催化活性与TiO_2的强化学吸附作用相结合，可以很好地稳定活性物质S，并有效减轻多硫化物的穿梭效应．该研究制备工艺简单、成本低廉，有望推动金属硫基电池的进一步发展和应用．

2.5 多级中空纤维在其他体系的应用

除了上述应用外，多级中空纤维材料还应用于其他类型二次电池领域：诸如金属空气电池、金属负极、锌电池和超级电容器等[104,105]．Wang等人[106]利用同轴静电纺丝结合热处理技术制备了一种Fe和Cu单原子分散的氮掺杂碳纳米纤维(Fe/Cu SAs)．通过引入Fe-N-C和Cu-N-C之间的非键相互作用来控制Fe中心的晶体场，然后在催化剂上施加外加磁场诱导自旋极化．铁原子的自旋状态可以从低自旋调节到中自旋和高自旋．高自旋Fe-N-C电催化剂具有较高的氧电催化活性，可以优化O_2的吸附，并加速决速步(*O_2到*OOH)的反应速率．高自旋Fe-N-C基可充电锌-空气电池具有170 mW cm^{-2}的高功率密度和良好的稳定性(图7(a))．

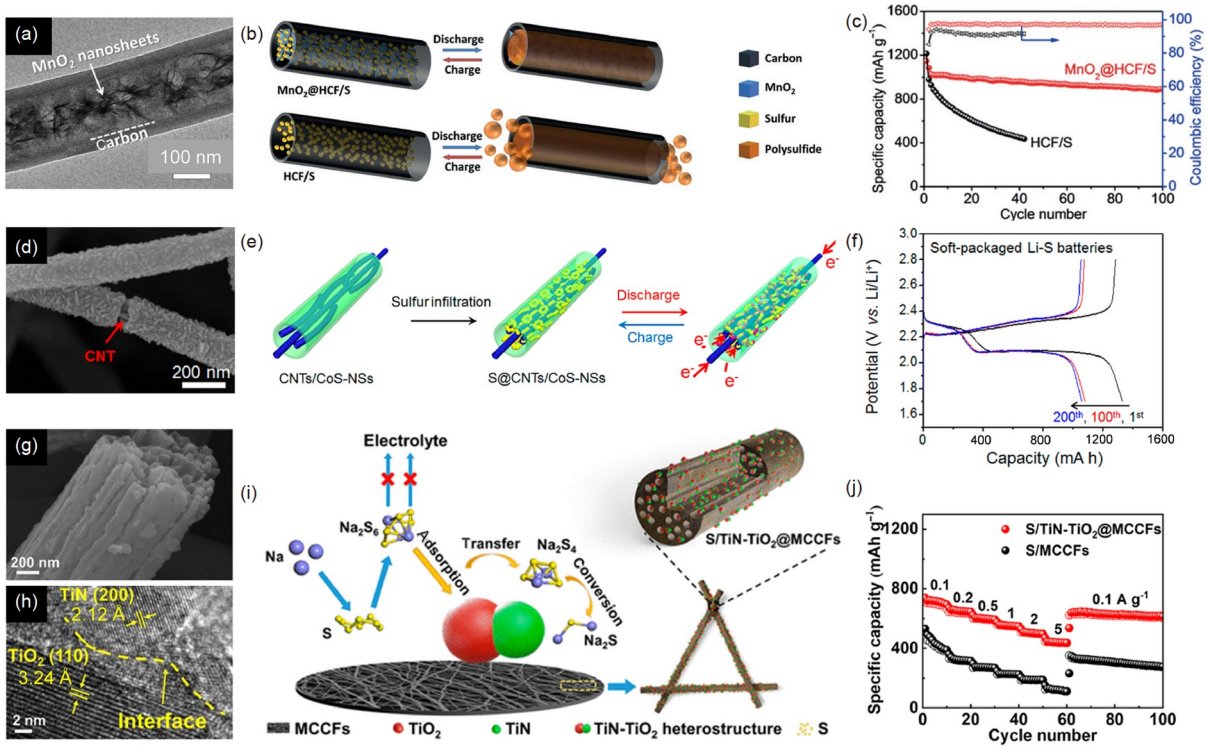


图 6 (网络版彩色)多级中空纤维用于锂/钠-硫电池. (a) MnO_2@HCF TEM图[101], Copyright©2015, John Wiley and Sons. (b) MnO_2@HCF/S和HCF/S的优势对比示意图. (c) MnO_2@HCF/S和HCF/S循环性能对比图. (d) CNTs/CoS-NSs形貌图[102], Copyright©2018, American Chemical Society. (e) S@CNTs/CoS-NSs制备图及反应机理图. (f) 充放电曲线. (g), (h) S/TiN-TiO_2@MCCFs形貌图[103], Copyright©2021, American Chemical Society. (i) S/TiN-TiO_2@MCCFs用于Na_2S_x吸附转化机理示意图. (j) 倍率性能图

Figure 6 (Color online) Multi-structure hollow nanofibers for lithium/sodium-sulfur batteries. (a) TEM image of MnO_2@HCF[101], Copyright©2015, John Wiley and Sons. (b) The comparative advantage diagram of MnO_2@HCF/S and HCF/S. (c) Cycle capacity of MnO_2@HCF/S in comparison with HCF/S. (d) The morphology of CNTs/CoS-NSs[102], Copyright©2018, American Chemical Society. (e) The formation and reaction mechanism of S@CNTs/CoS-NSs. (f) Discharge-charge profiles. (g), (h) The morphology of S/TiN-TiO_2@MCCFs[103], Copyright©2021, American Chemical Society. (i) Schematic diagram of the mechanism of S/TiN-TiO_2@MCCFs for Na_2S_x adsorption-conversion. (j) Rate performance

锂枝晶的生长和巨大的体积变化是制约锂金属负极实际应用的关键问题. 鉴于此, Chen等人[107]利用静电纺丝工艺制备了包裹有金属前体的PAN纤维, 在惰性气氛保护下对前驱体纤维进行热退火处理, 制得一种末端呈现莲藕状多孔结构的分级中空纤维, 即镍钴基中空棱柱/碳纤维材料(NCH@CFs)(图7(b), (c)). 将此纤维用作锂金属负极载体, 其高度分散的双金属Ni-Co颗粒均匀分布在N掺杂的碳纤维内外表面, 作为锂离子的成核位点有效降低锂成核过电势. 此外, 纤维呈现莲藕状分层中空结构, 可以有效防止电荷堆积、提高空间利用率、缓解体积膨胀、增强结构稳定性. 基于上述优点, NCH@CFs复合锂金属负极表现出优异的电化学性能. Li等人[108]开发了一种原位反应方法: 以金属有机框架(MOF)作为纳米反应器和成孔剂, 合成了由嵌入单分散锡团簇的氮掺杂碳纤维组成的介孔载体(Sn-NCNFs). 其表现出优异的亲钠性, 可实现快速的钠浸入和2 mV的超低钠成核过电位. 它的多孔结构保持了高钠含量, 并引导了均匀的钠沉积, 这些优势使得其具有优异的循环稳定性(图7(d)).

Li等人[109]运用静电纺丝技术制备了嵌有Sb纳米晶的3D柔性中空碳纤维复合骨架(Sb@HPCNF). Sb@HPCNF具有仿生"莲藕状"孔道结构(图7(e)), 其中, 插图为纤维3D模型图及实物的柔性展示照片. 它不仅显著改善了电极材料与电解液的浸润性, 而且大幅提升了活性位点的有效利用率. 更重要的是, 在界面处原位引入的表面官能团有效增强了金属Na的润湿性和亲和力, 驱使预沉积的钠离子流在Sb@HPCNF骨架表面优先成核, 大幅降低其形核能垒; 在体相中, 均匀锚定的Sb纳米晶与金属Na反应形成的Na_3Sb中间产物作为亲Na性更高的活性位点, 高效诱导了金属Na的稳定

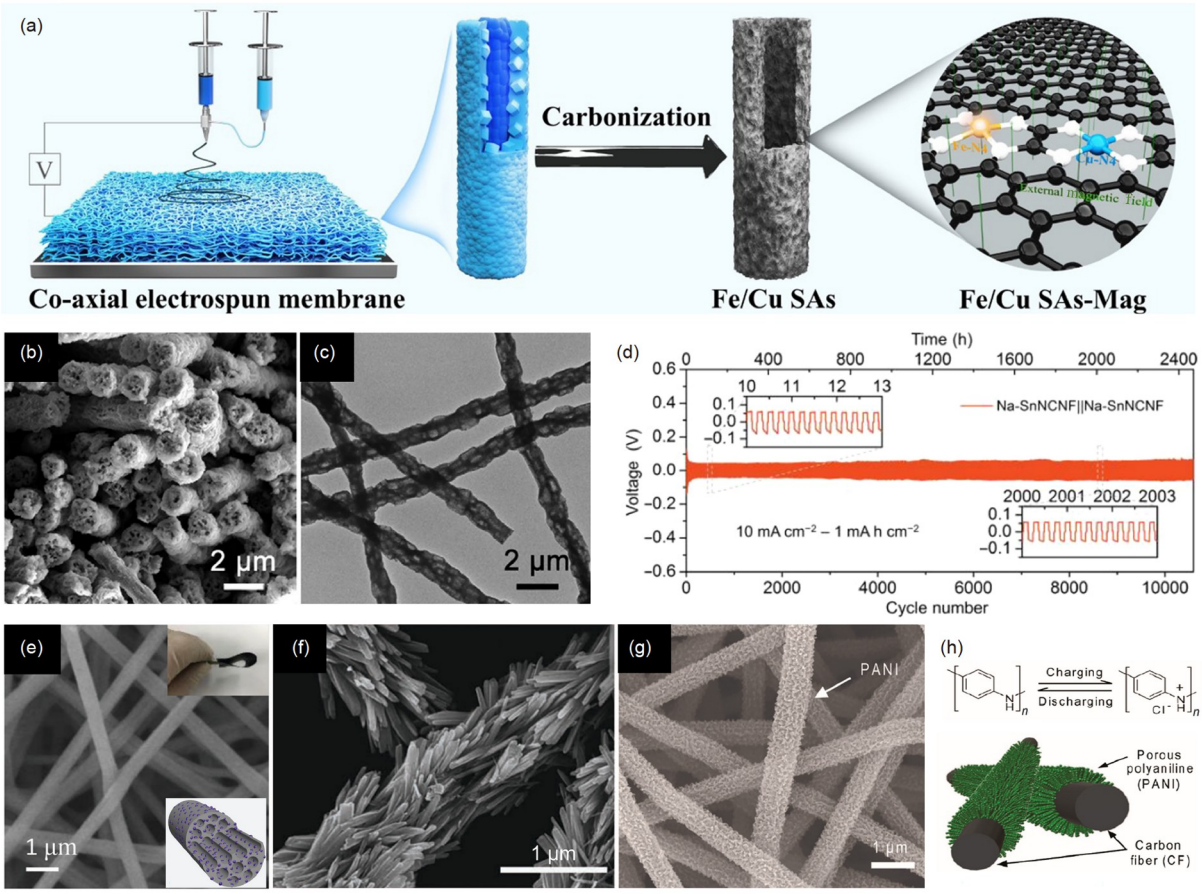


图 7 (网络版彩色)多级中空纤维在其他体系的应用. (a) Fe/Cu SAs合成示意图[106], Copyright©2023, John Wiley and Sons. (b), (c) 藕截面型NCH@CFs形貌图[107], Copyright©2021, John Wiley and Sons. (d) Na-SnNCNF||Na-SnNCNF电池循环性能图[108], Copyright©2023, John Wiley and Sons. (e) Sb@HPCNF纤维形貌图[109], Copyright©2023, John Wiley and Sons. (f) $MnMoO_4/CoMoO_4$分级异质纤维[110], Copyright©2011, Springer Nature. (g) PANI/CF形貌图[111], Copyright©2018, American Chemical Society. (h) 在苯胺水溶液中原位聚合合成PANI/CF正极示意图

Figure 7 (Color online) Multi-structure hollow fibers applications in other systems. (a) Schematic illustration of the synthesis of the Fe/Cu SAs[106], Copyright©2023, John Wiley and Sons. (b), (c) The morphology of lotus-root-like NCH@CFs[107], Copyright©2021, John Wiley and Sons. (d) Cycling performance of Na-SnNCNF||Na-SnNCNF[108], Copyright©2023, John Wiley and Sons. (e) The morphology of Sb@HPCNF[109], Copyright©2023, John Wiley and Sons. (f) $MnMoO_4/CoMoO_4$ hierarchical heterostructured fibers[110], Copyright©2011, Springer Nature. (g) The morphology of PANI/CF[111], Copyright©2018, American Chemical Society. (h) Schematic diagram illustrating the PANI/CF cathode synthesized by *in situ* polymerization in an aqueous aniline solution

沉积和水平生长. 得益于这种"双功能调控机制", 将其用作Na金属负极的集流体时, 在5 mA cm^{-2}下, Sb@HPCNF-Na对称电池能够高度可逆地运行超过550 h, 过电位低至24 mV. 将其与$Na_3V_2(PO_4)_3$正极组装成全电池, 在电流密度500 mA g^{-1}下经1000次充放电循环后的容量保持率高达93.7%, 并表现出良好的倍率性能.

除二次电池应用外, Mai等人[110]通过模板法和自组装法得到分级$MnMoO_4/CoMoO_4$异质纳米线(图7(f)). 基于分层$MnMoO_4/CoMoO_4$异质结构纳米线制备的非对称超级电容器在1 A g^{-1}电流密度下的比电容为187.1 F g^{-1}, 在1000次循环后的循环效率为98%, 显示出良好的可逆性. Iqbal等人[104]以炭黑掺杂碳纳米纤维/聚苯胺(PANI)核壳纳米纤维为原料, 经静电纺丝、炭化和电喷雾制备出了高柔性超级电容器电极材料, 在5000次循环后也能保持91%的优异电容. 此外, 在180°弯曲角度范围内, 超级电容器性能没有明显变化. Zhou等人[105]利用界面合成在纤维素纳米纤维(CNFs)上制备导电的金属-有机骨架纳米层(conductive metal-organic frameworks, c-MOFs), 形成CNF@c-MOF复合纳米纤维, 得到的复合纳米纤维展现出高达100 S cm^{-1}的电导率、分级微孔结构和优异的柔性. 这些结果进

一步表明, 构建分层多级结构可以大幅提升电容器的电化学性能. 此外, Kim等人[111]构建了分级异质的PANI涂层包裹碳纤维(PANI/CF)正极材料用于锌离子电池(图7(g), (h)). 首先, 通过静电纺丝技术合成柔性的碳纤维作为三维集流体. 然后, 将导电聚合物聚苯胺(一种有效的锌-聚苯胺电池正极材料)涂覆在碳纤维上, 得到所需的聚苯胺包裹碳纤维的正极材料. 分级结构的PANI/CF正极材料具有高表面积、优异的导电性和倍率性能. 除此之外, 相信多级中空纳米纤维材料在催化、载药、组织工程等方面也有较大应用潜力.

3 总结与展望

多级中空纳米纤维材料在二次电池电化学性能方面具有许多显著优势: (1) 多级中空结构可以提供大的比表面积、丰富的反应活性位点, 增加材料与电解液的接触面积, 缩短电/离子传输距离, 加速反应动力学; (2) 中空结构可提供适宜的空间, 缓冲充放电过程中材料的体积变化, 克服电极材料破碎、聚集问题, 拟制电池容量的衰减; (3) 中空结构纤维既可以作为活性物质(如S, Se, Li, Na, K等)的载体材料, 又可以自身作为活性物质参与氧化还原反应; (4) 一维纤维材料形成的三维导电网络有利于加速电子传输, 加速反应动力学. 这些独特的优势应用于二次电池时, 可获得优异的容量、倍率、循环性能. 因此, 对纤维材料结构和成分实现更精细的调控是未来发展的主要方向.

尽管多级中空纳米纤维材料具有上述的结构功能优势, 对于多级中空纳米纤维材料应用于二次电池而言, 仍然有一些问题并未得到有效解决: (1) 简单、规模化制备尺寸、结构均匀的多级中空纳米纤维的制备技术有待进一步开发. 传统的静电纺丝技术、水热法等大多只适用于实验室小规模制备, 无法满足工业化量产需求. 发展结构可控、成分可调的高产量、低成本多级中空纤维材料制备技术是非常必要的. (2) 多级中空纳米纤维材料在赋予活性物质高活性的同时, 也常常加速了副反应的进行, 如何实现与副反应的平衡协调也是需要解决的问题. (3) 多级中空结构材料相较于实心材料, 其体积能量密度相对较小. 因此, 如何控制材料适当的中空度是合成技术需要解决的重要问题. (4) 材料的孔径尺寸对电化学性能影响较大, 设计制备具有合适孔径的多级中空纳米纤维材料确实是未来发展的一个挑战. 如何根据材料的实际应用需求综合考虑孔径尺寸、电子传输、离子扩散和电极反应等因素以实现最佳的电化学性能是关键. (5) 多级中空纳米纤维因其结构、成分的复杂性, 其储能机制更为复杂, 如何对多层次结构和异质材料复合进行有效解耦是深入理解其电化学机理、反馈指导优化电极材料设计的重点和难点. 理解上述问题需要运用许多先进的原位、实时、高时空分辨表征手段对电极反应过程进行跟踪, 并结合计算化学进行材料筛选和机理揭示. (6) 目前的中空纤维结构制备技术普适性和规律性仍然不足, 许多材料的合成具有较多的偶然性因素, 如何按需定制具有精确组成、结构和尺寸的高效能电极材料仍然缺乏有效的指导方法. 未来人工智能、机器学习等技术有望为电极材料的按需定制提供更优化的合成路径, 减少试错成本. 因此, 随着多级中空纤维制备技术的进一步革新和理论认识的不断深入, 一维多级中空纳米纤维材料独特的结构和组成优势将在各种各样高效的电化学储能领域得到更加广泛的应用.

参考文献

1 Dunn B, Kamath H, Tarascon J M. Electrical energy storage for the grid: A battery of choices. Science, 2011, 334: 928–935
2 Lemoine K, Hémon-Ribaud A, Leblanc M, et al. Fluorinated materials as positive electrodes for Li- and Na-ion batteries. Chem Rev, 2022, 122: 14405–14439
3 Chu S, Majumdar A. Opportunities and challenges for a sustainable energy future. Nature, 2012, 488: 294–303
4 Obama B. The irreversible momentum of clean energy. Science, 2017, 355: 126–129
5 Liu Y, Zhu Y, Cui Y. Challenges and opportunities towards fast-charging battery materials. Nat Energy, 2019, 4: 540–550
6 Zhang X, Ju Z, Zhu Y, et al. Multiscale understanding and architecture design of high energy/power lithium-ion battery electrodes. Adv Energy Mater, 2021, 11: 2000808
7 Goodenough J B, Kim Y. Challenges for rechargeable Li batteries. Chem Mater, 2009, 22: 587–603
8 Choi J W, Aurbach D. Promise and reality of post-lithium-ion batteries with high energy densities. Nat Rev Mater, 2016, 1: 16013
9 Dang R B, Lu Y X, Rong X H, et al. Research progress of key materials and engineering exploration for Na-ion batteries (in Chinese). Chin Sci Bull, 2022, 67: 3546–3564 [党荣彬, 陆雅翔, 容晓晖, 等. 钠离子电池关键材料研究及工程化探索进展. 科学通报, 2022, 67: 3546–3564]

10 Sun Y, Liu N, Cui Y. Promises and challenges of nanomaterials for lithium-based rechargeable batteries. Nat Energy, 2016, 1: 16071
11 Li M, Lu J, Ji X, et al. Design strategies for nonaqueous multivalent-ion and monovalent-ion battery anodes. Nat Rev Mater, 2020, 5: 276–294
12 Zhang S, Ling F, Wang L, et al. An open-ended Ni_3S_2-Co_9S_8 heterostructures nanocage anode with enhanced reaction kinetics for superior potassium-ion batteries. Adv Mater, 2022, 34: 2201420
13 Yu X Y, Lou X W. Mixed metal sulfides for electrochemical energy storage and conversion. Adv Energy Mater, 2018, 8: 1701592
14 Xie F, Zhang L, Ye C, et al. The application of hollow structured anodes for sodium-ion batteries: From simple to complex systems. Adv Mater, 2019, 31: 1800492
15 Sun Y G, Cao A M. Recent development in self-templating approaches to hollow nanostructures and their electrochemical application (in Chinese). Chin Sci Bull, 2019, 64: 3607–3622 [孙勇刚, 曹安民. 基于自模板法构筑空心结构材料及其电化学应用. 科学通报, 2019, 64: 3607–3622]
16 Ma Y, Zhang L, Yan Z, et al. Sandwich-shell structured $CoMn_2O_4$/C hollow nanospheres for performance-enhanced sodium-ion hybrid supercapacitor. Adv Energy Mater, 2022, 12: 2103820
17 Bai S Y, Wang X Y, Liu Q L, et al. Construction of hollow structured carbon-based micro/nanoreactors (in Chinese). Chin Sci Bull, 2019, 64: 3562–3576 [白诗扬, 王昕尧, 刘庆隆, 等. 中空结构碳基微/纳米反应器的构筑. 科学通报, 2019, 64: 3562–3576]
18 Peng L, Peng H, Liu Y, et al. Spiral self-assembly of lamellar micelles into multi-shelled hollow nanospheres with unique chiral architecture. Sci Adv, 2021, 7: eabi7403
19 Xue J, Wu T, Dai Y, et al. Electrospinning and electrospun nanofibers: Methods, materials, and applications. Chem Rev, 2019, 119: 5298–5415
20 Wang J, Wang Z, Ni J, et al. Electrospinning for flexible sodium-ion batteries. Energy Storage Mater, 2022, 45: 704–719
21 Ding X B, Wu H L, Mo W B, et al. Synthetic method and application of the multi-shell hollow structure (in Chinese). Chin Sci Bull, 2019, 64: 3526–3545 [丁晓博, 吴华龙, 莫文彬, 等. 多壳层中空材料的制备及其应用. 科学通报, 2019, 64: 3526–3545]
22 Li Z, Wu H B, Lou X W. Rational designs and engineering of hollow micro-/nanostructures as sulfur hosts for advanced lithium-sulfur batteries. Energy Environ Sci, 2016, 9: 3061–3070
23 Zhou L, Zhuang Z, Zhao H, et al. Intricate hollow structures: Controlled synthesis and applications in energy storage and conversion. Adv Mater, 2017, 29: 1602914
24 Cheong J Y, Cho S, Lee J, et al. Multifunctional 1D nanostructures toward future batteries: A comprehensive review. Adv Funct Mater, 2022, 32: 2208374
25 Fang Y, Luan D, Gao S, et al. Rational design and engineering of one-dimensional hollow nanostructures for efficient electrochemical energy storage. Angew Chem Int Ed, 2021, 60: 20102–20118
26 Yan Z, Xiao J, Lai W, et al. Nickel sulfide nanocrystals on nitrogen-doped porous carbon nanotubes with high-efficiency electrocatalysis for room-temperature sodium-sulfur batteries. Nat Commun, 2019, 10: 4793
27 Wang Z, Peng S, Hu Y, et al. Cobalt nanoparticles encapsulated in carbon nanotube-grafted nitrogen and sulfur co-doped multichannel carbon fibers as efficient bifunctional oxygen electrocatalysts. J Mater Chem A, 2017, 5: 4949–4961
28 Li D, Xia Y. Direct fabrication of composite and ceramic hollow nanofibers by electrospinning. Nano Lett, 2004, 4: 933–938
29 Tian L, Ji D, Zhang S, et al. A humidity-induced nontemplating route toward hierarchical porous carbon fiber hybrid for efficient bifunctional oxygen catalysis. Small, 2020, 16: 2001743
30 Zhao Y, Cao X, Jiang L. Bio-mimic multichannel microtubes by a facile method. J Am Chem Soc, 2007, 129: 764–765
31 Li Z, Zhang J T, Chen Y M, et al. Pie-like electrode design for high-energy density lithium-sulfur batteries. Nat Commun, 2015, 6: 8850
32 Mou F, Guan J, Shi W, et al. Oriented contraction: A facile nonequilibrium heat-treatment approach for fabrication of maghemite fiber-in-tube and tube-in-tube nanostructures. Langmuir, 2010, 26: 15580–15585
33 Gao S, Wang N, Li S, et al. A multi-wall Sn/SnO_2@Carbon hollow nanofiber anode material for high-rate and long-life lithium-ion batteries. Angew Chem Int Ed, 2020, 59: 2465–2472
34 Chen H, Di J, Wang N, et al. Fabrication of hierarchically porous inorganic nanofibers by a general microemulsion electrospinning approach. Small, 2011, 7: 1779–1783
35 Li Z, Guan B Y, Zhang J, et al. A compact nanoconfined sulfur cathode for high-performance lithium-sulfur batteries. Joule, 2017, 1: 576–587
36 Pan Z, Chen H, Yang J, et al. $CuCo_2S_4$ nanosheets@N-doped carbon nanofibers by sulfurization at room temperature as bifunctional electrocatalysts in flexible quasi-solid-state Zn-air batteries. Adv Sci, 2019, 6: 1900628
37 Gao S, He Y, Yue G, et al. Pea-like MoS_2@$NiS_{1.03}$-carbon heterostructured hollow nanofibers for high-performance sodium storage. Carbon Energy, 2023, 5: e319
38 Huang H, Wang J, Yang X, et al. Unveiling the advances of nanostructure design for alloy-type potassium-ion battery anodes via *in situ* TEM. Angew Chem Int Ed, 2020, 59: 14504–14510
39 Fang Y, Zhang S L, Wu Z P, et al. A highly stable lithium metal anode enabled by Ag nanoparticle-embedded nitrogen-doped carbon

macroporous fibers. Sci Adv, 2021, 7: eabg3626
40 Zeng Y, Pei Z, Luan D, et al. Atomically dispersed zincophilic sites in N,P-codoped carbon macroporous fibers enable efficient Zn metal anodes. J Am Chem Soc, 2023, 145: 12333–12341
41 Liu Y, Chen X, Yu J, et al. Carbon-nanoplated CoS@TiO_2 nanofibrous membrane: An interface-engineered heterojunction for high-efficiency electrocatalytic nitrogen reduction. Angew Chem Int Ed, 2019, 58: 18903–18907
42 Niu C, Meng J, Wang X, et al. General synthesis of complex nanotubes by gradient electrospinning and controlled pyrolysis. Nat Commun, 2015, 6: 7402
43 Peng S, Li L, Hu Y, et al. Fabrication of spinel one-dimensional architectures by single-spinneret electrospinning for energy storage applications. ACS Nano, 2015, 9: 1945–1954
44 Wu Q, Xu R, Zhao R, et al. Tube-in-tube composite nanofibers with high electrochemistry performance in energy storage applications. Energy Storage Mater, 2019, 19: 69–79
45 Yu Y, Gu L, Zhu C, et al. Tin nanoparticles encapsulated in porous multichannel carbon microtubes: Preparation by single-nozzle electrospinning and application as anode material for high-performance Li-based batteries. J Am Chem Soc, 2009, 131: 15984–15985
46 Li D, Li H, Zheng S, et al. CoS_2-TiO_2@C core-shell fibers as cathode host material for high-performance lithium-sulfur batteries. J Colloid Interface Sci, 2022, 607: 655–661
47 Li S, Liu J, Ma L, et al. Okra-like multichannel TiO@NC fibers membrane with spatial and chemical restriction on shuttle-effect for lithium-sulfur batteries. Adv Fiber Mater, 2022, 5: 252–265
48 Feng L, Li S, Li H, et al. Super-hydrophobic surface of aligned polyacrylonitrile nanofibers. Angew Chem Int Ed, 2002, 41: 1221–1223
49 Jin R, Yang Y, Xing Y, et al. Facile synthesis and properties of hierarchical double-walled copper silicate hollow nanofibers assembled by nanotubes. ACS Nano, 2014, 8: 3664–3670
50 Ding Y L, Wen Y, Wu C, et al. 3D V_6O_{13} nanotextiles assembled from interconnected nanogrooves as cathode materials for high-energy lithium ion batteries. Nano Lett, 2015, 15: 1388–1394
51 Fan Z J, Yan J, Wei T, et al. Nanographene-constructed carbon nanofibers grown on graphene sheets by chemical vapor deposition: High-performance anode materials for lithium ion batteries. ACS Nano, 2011, 5: 2787–2794
52 Guan C, Wang X, Zhang Q, et al. Highly stable and reversible lithium storage in SnO_2 nanowires surface coated with a uniform hollow shell by atomic layer deposition. Nano Lett, 2014, 14: 4852–4858
53 Wang J, Wan J, Wang D. Hollow multishelled structures for promising applications: Understanding the structure-performance correlation. Acc Chem Res, 2019, 52: 2169–2178
54 Reddy M V, Subba Rao G V, Chowdari B V R. Metal oxides and oxysalts as anode materials for Li ion batteries. Chem Rev, 2013, 113: 5364–5457
55 Jin H, Xin S, Chuang C, et al. Black phosphorus composites with engineered interfaces for high-rate high-capacity lithium storage. Science, 2020, 370: 192–197
56 Zhao Y, Li X, Yan B, et al. Significant impact of 2D graphene nanosheets on large volume change tin-based anodes in lithium-ion batteries: A review. J Power Sources, 2015, 274: 869–884
57 Bi J, Du Z, Sun J, et al. On the road to the frontiers of lithium-ion batteries: A review and outlook of graphene anodes. Adv Mater, 2023, 35: 2210734
58 Mo R, Tan X, Li F, et al. Tin-graphene tubes as anodes for lithium-ion batteries with high volumetric and gravimetric energy densities. Nat Commun, 2020, 11: 1374
59 Kim C, Jung J W, Yoon K R, et al. A high-capacity and long-cycle-life lithium-ion battery anode architecture: Silver nanoparticle-decorated SnO_2/NiO nanotubes. ACS Nano, 2016, 10: 11317–11326
60 Wang X, Feng J, Bai Y, et al. Synthesis, properties, and applications of hollow micro-/nanostructures. Chem Rev, 2016, 116: 10983–11060
61 Jin J, Wu L, Huang S, et al. Hierarchy design in metal oxides as anodes for advanced lithium-ion batteries. Small Methods, 2018, 2: 1800171
62 Jung S K, Hwang I, Chang D, et al. Nanoscale phenomena in lithium-ion batteries. Chem Rev, 2019, 120: 6684–6737
63 Zhao L, Wu H H, Yang C, et al. Mechanistic origin of the high performance of yolk@shell Bi_2S_3@N-doped carbon nanowire electrodes. ACS Nano, 2018, 12: 12597–12611
64 Mao M, Yan F, Cui C, et al. Pipe-wire TiO_2-Sn@carbon nanofibers paper anodes for lithium and sodium ion batteries. Nano Lett, 2017, 17: 3830–3836
65 David L, Bhandavat R, Singh G. MoS_2/graphene composite paper for sodium-ion battery electrodes. ACS Nano, 2014, 8: 1759–1770
66 Luo W, Lorger S, Wang B, et al. Facile synthesis of one-dimensional peapod-like Sb@C submicron-structures. Chem Commun, 2014, 50: 5435–5437
67 Wen Y, He K, Zhu Y, et al. Expanded graphite as superior anode for sodium-ion batteries. Nat Commun, 2014, 5: 4033

68 Jiang Y, Wei M, Feng J, et al. Enhancing the cycling stability of Na-ion batteries by bonding SnS_2 ultrafine nanocrystals on amino-functionalized graphene hybrid nanosheets. Energy Environ Sci, 2016, 9: 1430–1438

69 Wu C, Dou S X, Yu Y. The state and challenges of anode materials based on conversion reactions for sodium storage. Small, 2018, 14: e1703671

70 Xie F, Zhang L, Gu Q, et al. Multi-shell hollow structured Sb_2S_3 for sodium-ion batteries with enhanced energy density. Nano Energy, 2019, 60: 591–599

71 Yabuuchi N, Kubota K, Dahbi M, et al. Research development on sodium-ion batteries. Chem Rev, 2014, 114: 11636–11682

72 Hwang J Y, Myung S T, Sun Y K. Sodium-ion batteries: Present and future. Chem Soc Rev, 2017, 46: 3529–3614

73 Goikolea E, Palomares V, Wang S, et al. Na-ion batteries—Approaching old and new challenges. Adv Energy Mater, 2020, 10: 2002055

74 Lee J M, Singh G, Cha W, et al. Recent advances in developing hybrid materials for sodium-ion battery anodes. ACS Energy Lett, 2020, 5: 1939–1966

75 Wang P F, Yao H R, Liu X Y, et al. Na^+/vacancy disordering promises high-rate Na-ion batteries. Sci Adv, 2018, 4: eaar6018

76 Ma D, Li Y, Mi H, et al. Robust SnO_{2-x} nanoparticle-impregnated carbon nanofibers with outstanding electrochemical performance for advanced sodium-ion batteries. Angew Chem Int Ed, 2018, 57: 8901–8905

77 Pan Q, Zhang Q, Zheng F, et al. Construction of MoS_2/C hierarchical tubular heterostructures for high-performance sodium ion batteries. ACS Nano, 2018, 12: 12578–12586

78 Yuan J, Qiu M, Hu X, et al. Pseudocapacitive vanadium nitride quantum dots modified one-dimensional carbon cages enable highly kinetics-compatible sodium ion capacitors. ACS Nano, 2022, 16: 14807–14818

79 Ge J M, Fan L, Wang J, et al. $MoSe_2$/N-doped carbon as anodes for potassium-ion batteries. Adv Energy Mater, 2018, 8: 1801477

80 Ding J, Zhang H, Zhou H, et al. Sulfur-grafted hollow carbon spheres for potassium-ion battery anodes. Adv Mater, 2019, 31: 1900429

81 Cui Y, Liu W, Feng W, et al. Controlled design of well-dispersed ultrathin MoS_2 nanosheets inside hollow carbon skeleton: Toward fast potassium storage by constructing spacious “houses” for K ions. Adv Funct Mater, 2020, 30: 1908755

82 Lim J B, Kim M, Park S K. Construction of N-doped multichannel carbon nanofibers embedded with amorphous VS_4 nanoparticles for potassium-ion batteries with ultralong-term cycling stability. Appl Surf Sci, 2022, 602: 154332

83 Li W, Wang D, Gong Z, et al. A robust strategy for engineering Fe_7S_8/C hybrid nanocages reinforced by defect-rich MoS_2 nanosheets for superior potassium-ion storage. ACS Nano, 2020, 14: 16046–16056

84 Hu R, Sha D, Cao X, et al. Anchoring metal-organic framework-derived ZnTe@C onto elastic $Ti_3C_2T_x$ MXene with 0D/2D dual confinement for ultrastable potassium-ion storage. Adv Energy Mater, 2022, 12: 2203118

85 Xiao Y, Liu F, Shi H, et al. Construction of ultrastable ultrathin black phosphorus nanodisks hybridized with Fe_3O_4 nanoclusters and iron (V)-Oxo complex for efficient potassium storage. Adv Mater, 2023, 2301772

86 Yuan T, Yan J, Zhang Q, et al. Unveiling the nature of ultrastable potassium storage in $Bi_{0.48}Sb_{1.52}Se_3$ composite. ACS Nano, 2023, 17: 10462–10473

87 Jia B, Yu Q, Zhao Y, et al. Bamboo-like hollow tubes with MoS_2/N-doped-C interfaces boost potassium-ion storage. Adv Funct Mater, 2018, 28: 1803409

88 Yi Z, Jiang S, Tian J, et al. Amidation-dominated re-assembly strategy for single-atom design/nano-engineering: Constructing Ni/S/C nanotubes with fast and stable K-storage. Angew Chem Int Ed, 2020, 59: 6459–6465

89 Li Q, Peng J, Zhang W, et al. Manipulating the polytellurides of metallic telluride for ultra-stable potassium-ion storage: A case study of carbon-confined $CoTe_2$ nanofibers. Adv Energy Mater, 2023, 13: 2300150

90 Wang Y X, Yang J, Chou S L, et al. Uniform yolk-shell iron sulfide-carbon nanospheres for superior sodium-iron sulfide batteries. Nat Commun, 2015, 6: 8689

91 Seh Z W, Sun Y, Zhang Q, et al. Designing high-energy lithium-sulfur batteries. Chem Soc Rev, 2016, 45: 5605–5634

92 Dong C, Gao W, Jin B, et al. Advances in cathode materials for high-performance lithium-sulfur batteries. iScience, 2018, 6: 151–198

93 Fu A, Wang C, Pei F, et al. Recent advances in hollow porous carbon materials for lithium-sulfur batteries. Small, 2019, 15: 1804786

94 Lei Y, Wu C, Lu X, et al. Streamline sulfur redox reactions to achieve efficient room-temperature sodium-sulfur batteries. Angew Chem Int Ed, 2022, 61: e202200384

95 Xiong R D, Xiang J W, Li X, et al. Synergistic improvement of the overall performance of lithium-sulfur batteries (in Chinese). Chin Sci Bull, 2022, 67: 1072–1087 [熊润荻, 向经纬, 李想, 等. 锂硫电池综合性能协同提升策略. 科学通报, 2022, 67: 1072–1087]

96 Zhu Z, Zeng Y, Pei Z, et al. Bimetal-organic framework nanoboxes enable accelerated redox kinetics and polysulfide trapping for lithium-sulfur batteries. Angew Chem Int Ed, 2023, 62: e202305828

97 Zhou W, Ning S, Fan B, et al. One-dimensional confined p-n junction Co_3S_4/MoS_2 interface nanorods significantly enhance polysulfide redox kinetics for Li-S batteries. J Mater Chem A, 2023, 11: 926–936

98 Zhang L, Li T, Zhang X, et al. Core-shell polyoxometalate-based zeolite imidazole framework-derived multi-interfacial $MoSe_2$/$CoSe_2$@NC

enabling multi-functional polysulfide anchoring and conversion in lithium-sulfur batteries. J Mater Chem A, 2023, 11: 3105–3117
99 Zhang S, Yao Y, Jiao X, et al. Mo_2N-W_2N heterostructures embedded in spherical carbon superstructure as highly efficient polysulfide electrocatalysts for stable room-temperature Na-S batteries. Adv Mater, 2021, 33: 2103846
100 Zhou F, Li Z, Luo X, et al. Low cost metal carbide nanocrystals as binding and electrocatalytic sites for high performance Li-S batteries. Nano Lett, 2018, 18: 1035–1043
101 Li Z, Zhang J, Lou X W. Hollow carbon nanofibers filled with MnO_2 nanosheets as efficient sulfur hosts for lithium-sulfur batteries. Angew Chem Int Ed, 2015, 54: 12886–12890
102 Ma L, Zhang W, Wang L, et al. Strong capillarity, chemisorption, and electrocatalytic capability of crisscrossed nanostraws enabled flexible, high-rate, and long-cycling lithium-sulfur batteries. ACS Nano, 2018, 12: 4868–4876
103 Ye X, Ruan J, Pang Y, et al. Enabling a stable room-temperature sodium-sulfur battery cathode by building heterostructures in multichannel carbon fibers. ACS Nano, 2021, 15: 5639–5648
104 Iqbal N, Wang X, Babar A A, et al. Polyaniline enriched flexible carbon nanofibers with core-shell structure for high-performance wearable supercapacitors. Adv Mater Inter, 2017, 4: 1700855
105 Zhou S, Kong X, Zheng B, et al. Cellulose nanofiber@conductive metal-organic frameworks for high-performance flexible supercapacitors. ACS Nano, 2019, 13: 9578–9586
106 Wang Y, Meng P, Yang Z, et al. Regulation of atomic Fe-spin state by crystal field and magnetic field for enhanced oxygen electrocatalysis in rechargeable zinc-air batteries. Angew Chem Int Ed, 2023, 62: e202304229
107 Chen C, Guan J, Li N W, et al. Lotus-root-like carbon fibers embedded with Ni-Co nanoparticles for dendrite-free lithium metal anodes. Adv Mater, 2021, 33: 2100608
108 Li S, Zhu H, Liu Y, et al. Space-confined guest synthesis to fabricate Sn-monodispersed N-doped mesoporous host toward anode-free Na batteries. Adv Mater, 2023, 35: 2301967
109 Li Z, Qin H, Tian W, et al. 3D Sb-based composite framework with gradient sodiophilicity for ultrastable sodium metal anodes. Adv Funct Mater, 2023, 2301554
110 Mai L Q, Yang F, Zhao Y L, et al. Hierarchical $MnMoO_4$/$CoMoO_4$ heterostructured nanowires with enhanced supercapacitor performance. Nat Commun, 2011, 2: 381
111 Kim C, Ahn B Y, Wei T S, et al. High-power aqueous zinc-ion batteries for customized electronic devices. ACS Nano, 2018, 12: 11838–11846

Summary for “多级中空纳米纤维二次电池电极材料”

Multi-structure hollow nanofibers electrode materials for secondary batteries

Songwei Gao[1], Wei Guo[1], Yue Mu[1], Keping Zhu[1], Zhimin Cui[1], Xingkun Man[2], Qianfan Zhang[3], Nü Wang[1*] & Yong Zhao[1*]

[1] *Beijing Key Laboratory of Bioinspired Energy Materials and Devices, Key Laboratory of Bioinspired Smart Interfacial Science and Technology of Ministry of Education, School of Chemistry, Beihang University, Beijing 100191, China;*
[2] *School of Physics, Beihang University, Beijing 100191, China;*
[3] *School of Materials Science and Engineering, Beihang University, Beijing 100191, China*
* Corresponding authors, E-mail: wangn@buaa.edu.cn; zhaoyong@buaa.edu.cn

With the diversified development of human energy consumption, traditional fossil energy such as coal, oil and natural gas can no longer satisfy people’s needs for industry and high quality life. Furthermore, the use of these energy sources often leads to severe environmental pollution. The emergence of clean energy sources like wind energy, water energy and solar energy not only effectively alleviates the issues of energy scarcity and environmental pollution but also promises a cleaner, healthier, and more sustainable future for global society. However, the efficient storage and utilization of these clean energy sources have become particularly crucial. The development of the new clean energy has continuously stimulated researchers to explore advanced devices for the electrochemical energy storage. Secondary battery has many advantages in electrochemical energy storage technology, such as portability and flexibility, high energy conversion efficiency and environmental friendliness, and is considered to be one of the most promising energy storage technologies at present. Therefore, the development of efficient new energy secondary batteries is the important way to achieve the goal of “carbon peak and carbon neutrality”.

As typical representatives of new-generation secondary batteries, lithium-ion and sodium-ion batteries play significant roles in our daily lives. Especially with the improvement of human living standards, there are higher demands for battery capacity, rate performance, and long-term cycling stability. In recent years, it has been discovered that the reasonable design of the structure and composition for anode/cathode materials is the key to achieve high performance secondary batteries. Structural design can significantly enhance the effective capacity and long-term cycling stability of existing materials. The design of electrode material composition can achieve synergistic effects between multiple components, enabling efficient redox reactions. Multi-structure hollow nanofiber materials have the advantages of controllable structure and adjustable composition, and are widely used as electrode materials for secondary batteries. In terms of structure, the multi-structure hollow nanostructure effectively alleviates the volume change of the electrode material in the electrochemical reaction process, prevents the electrode material pulverization and aggregation, increases the effective contact area between the electrolyte and the electrode material, and shorters the ion/electron transport path. In terms of composition, it is easy to achieve reasonable coupling of materials with different characteristics, so as to achieve specific adsorption of different materials, improve the conductivity of electrode materials, and accelerate the kinetics of redox reaction.

In this review, representative methods for preparing multi-structure hollow nanofibers are summarized, including single-needle electrospinning, multi-fluid electrospinning and other synthesis methods (template method, hydrothermal method, and self-assembly method, etc.). Subsequently, we have summarized the application progresses of multi-structure hollow fibers with different structures and compositions in secondary batteries (including lithium-/sodium-/potassium-ion batteries, lithium/sodium-sulfur batteries, lithium-metal/air batteries, supercapacitors, etc.). Finally, we present the challenges and the application potential on the future research of multi-structure hollow nanofiber materials in the field of electrochemical energy storage.

multi-structure hollow structure, nanofiber, heterostructure, secondary batteries, electrode materials

doi: 10.1360/TB-2023-0887